Assessing the Role of Fluorine in the Performance of $Al_xGa_{1-x}N$/GaN High-Electron-Mobility Transistors from First-Principles Calculations

Rong Wang,[1,2,*] Xiaodong Tong,[1,2] Jianxing Xu,[1,2] Shiyong Zhang,[1,2] Penghui Zheng,[1,2] Feng-Xiang Chen,[3] and Wei Tan[1,2,†]

[1] *Microsystem and Terahertz Research Center, China Academy of Engineering Physics, Chengdu 610200, China*
[2] *Institute of Electronic Engineering, China Academy of Engineering Physics, Mianyang 621999, China*
[3] *Department of physics, School of Science, Wuhan University of Technology, Wuhan 430070, China*

(Received 17 December 2018; revised manuscript received 17 March 2019; published 8 May 2019)

Doping fluorine (F) into the $Al_xGa_{1-x}N$ layer is critical to the performance of enhancement-mode $Al_xGa_{1-x}N$/GaN high-electron-mobility transistors (HEMTs). However, the understanding of the role of F in $Al_xGa_{1-x}N$/GaN HEMTs is rather limited. Using the first-principles-calculated defect formation energies and transition energy levels, combined with the special quasirandom structure approach and the detailed balance theory, we investigate the interaction between F and native defects and impurities, as well as its effect on the Fermi energy of the $Al_xGa_{1-x}N$ alloy. Our results suggest that F is incorporated as F_i^- in the $Al_xGa_{1-x}N$ layer, which exhibits auto *n*-type conductivity because of unintentionally induced oxygen (O). F doping causes the redistribution of the charge states of intrinsic defects and impurities, and thus the Fermi energy of the $Al_xGa_{1-x}N$ layer. The charge-redistribution depends on the difference between the concentrations of F and O. Finally, we reveal the mechanism for the change of the electronical performance of $Al_xGa_{1-x}N$/GaN HEMTs after F doping. The positive shift of the threshold voltage is related to the negatively charged F_i. Only when the concentration of F is higher than that of unintentionally induced O in $Al_xGa_{1-x}N$, F begins to increase the surface potential and the Schottky barrier height of $Al_xGa_{1-x}N$/GaN HEMTs.

DOI: 10.1103/PhysRevApplied.11.054021

I. INTRODUCTION

$Al_xGa_{1-x}N$/GaN have long been viewed as promising materials for next-generation high-electron-mobility transistors (HEMTs), which are remarkable candidates for microwave power amplifiers and high-speed digital circuits [1–3]. One of the limits in these applications stems from the negative threshold voltage (V_{th}), which complicates circuit configurations, increases system costs, and poses safety concerns [4]. Incorporation of fluorine (F) into the $Al_xGa_{1-x}N$ layer was utilized to positively shift the V_{th} and the realization of the enhancement-mode or normally off HEMTs [5,6].

Experimentally, it was found that carbon tetrafluoride (CF_4) plasma, sulfur-hexafluoride (SF_6) plasma, and $^{19}F^+$-ion implantation could introduce F throughout the $Al_xGa_{1-x}N$ layer [7–12]. F was proposed to present as interstitial F (F_i) [6,13,14], substitutional F at N sites (F_N) [15], or substitutional F at group-III-atom sites (F_{Al} and F_{Ga}) [16,17]. One of the researches indicated that the positive shift of the V_{th} is accompanied by slight increases of the surface potential and the Schottky barrier height [18]. The mechanism for the V_{th} modulation was proposed under the assumption that negatively charged F_i dominates the defect configuration of F [14]. The negatively charged F_i was thought to upward bend the conduction band (CB) of the $Al_xGa_{1-x}N$ layer and raise its conduction-band minimum (CBM) above the Fermi level [14]. First, the assumption of the negatively charged F_i was based on the high electronegativity of F. First-principles calculations have indicated that high electronegative chlorine (Cl) could be positively charged in CdTe [19,20]. Therefore, the stable charge state of F_i needs to be addressed. Second, the defect configuration and its stable charge state rely on both the electron Fermi energy and the chemical potential of each constituent [21–23]. It may not be complete to directly assume the formation of negatively charged F_i. Moreover, although the V_{th} modulation is well explained by the mechanism, the reason for the increases of the surface potential and Schottky barrier height is still ambiguous. Theoretically, the formation energies of F_N and F_i were investigated in GaN and AlN [24,25]. We should note that the alloying effect of $Al_xGa_{1-x}N$, which plays an important role in the incorporation and ionization of defects, should not be neglected.

*wangrong@mtrc.ac.cn
†tanwei@mtrc.ac.cn

Clearly, the understanding on the role of F in $Al_xGa_{1-x}N$/GaN HEMTs concerns the defect physics of F in the $Al_xGa_{1-x}N$ alloy, the interaction between F and native defects and impurities, as well as its effect on the Fermi level of the host compound. To deal with these issues, we use the first-principles-calculated defect-formation energies and transition energy levels, combined with the special quasirandom structure (SQS) approach and the detailed balance theory to study the defect physics of F in $Al_{0.25}Ga_{0.75}N$, investigate the mechanism for the change of electronical performance of $Al_xGa_{1-x}N$/GaN HEMTs after F doping. We confirm that oxygen (O) will dope GaN and $Al_xGa_{1-x}N$ alloys to be *n*-type [26,27]. Therefore, if O is present in significant quantities in GaN and $Al_xGa_{1-x}N$ alloys, it will result in unintentional *n*-type conductivity. For *n*-type $Al_{0.25}Ga_{0.75}N$ with unintentionally induced O, when the concentration of F is lower than that of ionized O, the effect of F_i^- on the Fermi energy is negligible. Once the concentration of F becomes comparable or even larger than that of ionized O, the Fermi energy of $Al_{0.25}Ga_{0.75}N$ decreases rapidly with the increase of the F concentration. We find the positive shift of the V_{th} is related to F_i^-. The changes of the surface potential and Schottky barrier height depend on the concentration of incorporated F. Only when the concentration of F is higher than that of unintentionally induced O, F begins to increase the surface potential and the Schottky barrier height.

II. THEORETICAL DESCRIPTION

In this work, we take $Al_{0.25}Ga_{0.75}N$ as an example to investigate the effect of F doping on the electronic properties of $Al_xGa_{1-x}N$/GaN HEMTs, given the fact that the Al composition of the $Al_xGa_{1-x}N$ layer is usually in the range of 20%–30%. The calculations of the formation energies of F are carried out in the 96-atom special quasirandom structure of $Al_{0.25}Ga_{0.75}N$ [28–31]. In the SQS of $Al_{0.25}Ga_{0.75}N$, the probability of finding a N site with the first-neighbor motif Al_nGa_{4-n} is $p_n(x) = C_4^n x^n (1-x)^{4-n}$ ($x = 0.25$), which is the same as that in a perfectly random $Al_{0.25}Ga_{0.75}N$ [32].

First-principles total-energy calculations are performed using the hybrid density-functional proposed by Heyd, Scuseria, and Ernzerhof (HSE) for the exchange correlation and the projector-augmented wave (PAW) pseudopotentials as implemented in the Vienna *ab initio* simulation package (VASP) [33,34]. The Ga *3d* states are included as valence electrons in the pseudopotentials. In HSE, the fraction of screened Fock exchange is 0.32 [35]. The Brillouin zone integration is sampled with a $2 \times 2 \times 2$ Γ-centered Monkhorst-Pack special *k*-point mesh [36].

During the defect-formation-energy calculations, we adopt the mixed *k*-point scheme [21], which benefits from both gaining accurate structural relaxation energies by the special *k*-point approach and gaining accurate defect levels by the Γ-point-only approach. The formation energy of a defect α at the charge state q [$\Delta H_f(\alpha,q)$] as a function of the atomic potential μ_i and the electron Fermi energy E_F is calculated by [37,38]

$$\Delta H_f(\alpha,q) = \Delta E(\alpha,q) + \sum n_i \mu_i + qE_F, \qquad (1)$$

where $\Delta E(\alpha,q) = E(\alpha,q) - E(\text{host}) + n_i E_i + qE_{\text{VBM}}$, $E(\text{host})$, and $E(\alpha,q)$ are the total energies of the host and the host containing the defect α with charge state q, respectively. The total energies of charged systems are calculated by adding or subtracting charges to a virtual state with an average energy E_F, and a plane-wavelike compensating jellium background in the supercell is assumed to preserve the neutrality of the supercell. n_i is the number of atom i transferred from the supercell to the reservoir during the formation the defect α, μ_i is the chemical potential of the constituent i referenced to its elemental solid-gas with energy E_i, E_F is the Fermi energy referenced to the valance-band maximum (VBM) of the host.

It is known that the alloying effect causes both the band-edge shift and the bowing of defect formation energies in semiconductor alloys [28,32]. In order to take the alloying effect of $Al_{0.25}Ga_{0.75}N$ into account, we calculate the effective formation energies of V_N, O_N, F_i, and F_N in the $Al_{0.25}Ga_{0.75}N$ supercell. Given the localized character for the wave function around the defect's site, the defect properties are sensitive to its local environment. For F_N, V_N, and O_N in $Al_{0.25}Ga_{0.75}Ne$ local motif is their four-neighboring group-III atoms, which could be Al_xGa_{4-x} ($x = 0 \sim 4$) [28]. We find the site dependence for the formation energies of F_N, V_N, and O_N is smaller than 0.05 eV as long as they have the same local motif. Therefore, we calculate the formation energies of F_N, V_N, and O_N with five representative local motifs [Al_xGa_{4-x} ($x = 0 \sim 4$)], take the weighted average of them for the calculation of the effective formation energies of F_N, V_N, and O_N in $Al_{0.25}Ga_{0.75}N$. The local motif of F_i in $Al_{0.25}Ga_{0.75}N$ is Al_xGa_{3-x} ($x = 0 \sim 3$). We find the formation energies of F_i with the same local motif on different sites are widely distributed [28]. Therefore, we calculate the formation energies of F_i at all sites in $Al_{0.25}Ga_{0.75}N$ for the calculation of the effective formation energy of F_i in $Al_{0.25}Ga_{0.75}N$. At the temperature T, the effective formation energy $\Delta H_{\text{eff}}(\alpha,T)$ of a defect α is calculated by

$$\exp[-\Delta H_{\text{eff}}(\alpha,T)/k_B T] = \frac{1}{N}\sum_s \exp[-\Delta H_f(\alpha,s)/k_B T], \qquad (2)$$

where $\Delta H_f(\alpha,s)$ is the formation energy of defect α at the site s, k_B is the Boltzmann constant, N is the total number of site s in the $Al_{0.25}Ga_{0.75}N$ supercell.

We use F_N and F_i as examples to examine the convergence of neutral and charged-defect formation energies

with respect to the supercell size. For F_N with the local motif of Al_1Ga_3, increasing from the 96-atom supercell to the 192-atom supercell results in changes of the formation energies of F_N by less than 0.04 eV. The formation energies of F_i with the same local motif on different sites are widely distributed, it is difficult to compare the formation energy convergence of F_i in $Al_{0.25}Ga_{0.75}N$. Therefore, we compare the neutral and charged formation energies of F_i in 96-atom and 256-atom GaN supercells. The increase of supercell size changes the formation energies of F_i by less than 0.07 eV. The changes in the formation energies would not change the relative stability order for defects in $Al_{0.25}Ga_{0.75}N$. These results indicate that the 96-atom supercell is sufficient to converge defect formation energies in this work.

Based on first-principles-calculated formation energies and the electronic structures of F, we use the detailed balance theory to investigate the effect of F on the Fermi energy of $Al_xGa_{1-x}N$ [38]. The calculations are based on the requirement of the charge neutrality condition:

$$p_0 + \sum_i q_i N_{D_i}^{q_i^+} = n_0 + \sum_j q_j N_{A_j}^{q_j^-}, \tag{3}$$

where p_0 and n_0 are the concentrations of thermally excited holes and electrons, respectively. $N_{D_i}^{q_i^+}$ is the density of a donor D_i with the charge state q_i^+, $N_{A_j}^{q_j^-}$ is the density of an acceptor A_j with the charge state q_j^-. At a given temperature, p_0 and n_0 are given by

$$\begin{aligned} p_0 &= N_V e^{(E_V - E_F)/k_B T}, \\ n_0 &= N_C e^{-(E_C - E_F)/k_B T}. \end{aligned} \tag{4}$$

Here $N_V = 2(2\pi m_p^* k_B T)^{3/2}/h^3$ and $N_C = 2(2\pi m_n^* k_B T)^{3/2}/h^3$ are the effective density of states for valence bands and conduction bands, respectively. m_p^* ($1.02m_0$ for $Al_{0.25}Ga_{0.75}N$) and m_n^* ($0.22m_0$ for $Al_{0.25}Ga_{0.75}N$) are effective masses of holes and electrons, respectively [39]. k_B is the Boltzmann constant, h is the Planck constant. E_V and E_C are the energies of the VBM and CBM, respectively. Based on HSE calculations, we set $E_V = 0$ eV and $E_C = E_g = 3.97$ eV for $Al_{0.25}Ga_{0.75}N$. The concentration for a defect α with charge state q is calculated by

$$N(\alpha, q) = N_{\text{site}} g_q e^{-\Delta H_f(\alpha,q)/k_B T}. \tag{5}$$

Here N_{site} is the number of possible sites per volume for the defect α, g_q is the degeneracy factor related to possible electron configurations [38]. By solving Eqs. (1)–(5), we can get the Fermi energy of a host compound at given temperature and chemical potentials.

III. RESULTS AND DISCUSSION

A. Formation energies of defects

Figure 1 shows the effective formation energies of F_N and F_i in $Al_{0.25}Ga_{0.75}N$. The native defects of V_N, V_{Al}, and V_{Ga} in $Al_{0.25}Ga_{0.75}N$ are considered. It is widely accepted that O gives rise to the auto *n*-type conductivity of GaN [26,27]. Therefore, the dominant defect configuration of O_N for O is also under consideration. Given the localization for the wave function of a defect around its site, the defect properties are sensitive to its local environment. For F_N, V_N, O_N, and F_i, the local motifs are the neighboring group-III atoms, which differs from site to site. Therefore, we calculate the effective formation energies of F_N, V_N, O_N, and F_i to take the alloying effect into account. The temperature is set to be 1400 K, which is typical for the growth and annealing of $Al_xGa_{1-x}N$.

Similar to the defect properties of F in GaN/AlN [24,25], F_N^{2+} and F_i^- dominant the defect configurations of F in *p*-type and *n*-type $Al_{0.25}Ga_{0.75}N$, respectively. The charge state of F_N changes directly from 2+ to 0 when the Fermi energy increases throughout the bandgap of $Al_{0.25}Ga_{0.75}N$. During the charge transition, the F atom displaces from the original N site, results in a distorted structure and decreases the structural symmetry. This process is similar to the charge transition of F_N in GaN/AlN [24,25,28].

Previous works indicated that F_i is a shallow acceptor in GaN/AlN, where neutral and negatively charged F_i both locate at the channel-centered site [24,25]. In this work, we examine the possible formation of positively charged F_i. It turns out that F_i^+ forms the "N-F split interstitial" at the N site, which is similar to the nitrogen split interstitial in GaN. The distorted structure gives rise to the splitting

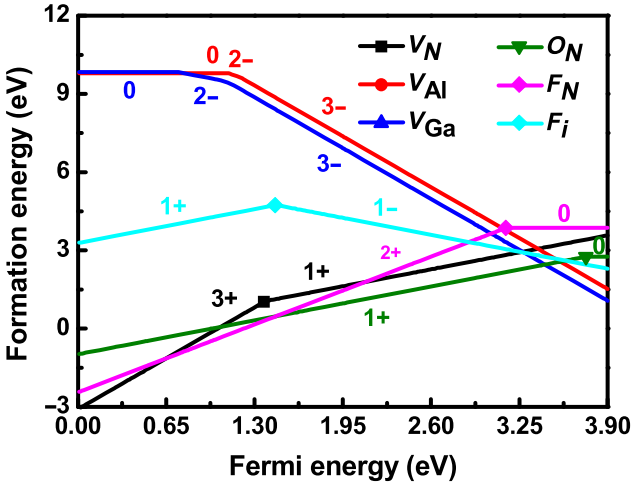

FIG. 1. Calculated formation energies of V_{Al} and V_{Ga}, effective formation energies of V_N, O_N, F_N, and F_i at 1400 K in $Al_{0.25}Ga_{0.75}N$ at the Ga-rich limit. The stable charge states of each defect are included in the figure.

of electron levels of F_i. Because the electronic energy gain resulted from the level splitting prevails over the energy cost of forming the distorted structure [19,20], the positively charged F_i is stabilized as the "N-F split interstitial" at the N site. We can see from Fig. 1 that F_i behaves as a negative-U center in $Al_{0.25}Ga_{0.75}N$.

The slight difference for the formation energies of V_{Al} and V_{Ga} in $Al_{0.25}Ga_{0.75}N$ is because the alloy concentration changes more after removing an Al atom (compared with the case removing a Ga atom) from the supercell.

B. Fermi level of $Al_{0.25}Ga_{0.75}N$ before F doping

We first calculate the Fermi energy of $Al_{0.25}Ga_{0.75}N$ with native defects (intrinsic dominant defects of V_N, V_{Al}, V_{Ga}, and inevitably induced O_N) that unintentionally induced during the growth. It can be seen from Fig. 1 that the formation energy of O_N is lower than those of V_N, V_{Al}, and V_{Ga} in a wide range of Fermi energy. Therefore, we investigate the effect of O_N on the Fermi energy of $Al_{0.25}Ga_{0.75}N$. The Fermi energy of $Al_{0.25}Ga_{0.75}N$ containing O_N is decided by O_N, V_N, V_{Al}, and V_{Ga}. The formation energy of O_N at various charge states are given by

$$\begin{aligned}\Delta H_f(\mathrm{O_N},0) &= E(\mathrm{O_N},0) - E(\mathrm{Al_{0.25}Ga_{0.75}N}) \\ &\quad + [\mu_N + E(\mathrm{N})] - [\mu_O + E(\mathrm{O})] \\ \Delta H_f(\mathrm{O_N},+) &= \Delta H_f(\mathrm{O_N},0) + \epsilon(0/+) - E_g + E_F. \quad (6)\end{aligned}$$

The concentrations of O_N in various charge states [$N(O_N,0)$ and $N(O_N,+)$] are calculated by Eq. (5). If there are totally $N(O_N)$ in $Al_{0.25}Ga_{0.75}N$, we have

$$\mathrm{N(O_N)} = \mathrm{N(O_N},0) + \mathrm{N(O_N},+). \quad (7)$$

With Eqs. (5)–(7), we have

$$\begin{aligned}\mathrm{N(O_N},0) &= \frac{2\mathrm{N(O_N)}}{2 + e^{-[\varepsilon(0/+)-E_g+E_F]/k_BT}}, \\ \mathrm{N(O_N},+) &= \frac{\mathrm{N(O_N)}e^{-[\varepsilon(0/+)-E_g+E_F]/k_BT}}{2 + e^{-[\varepsilon(0/+)-E_g+E_F]/k_BT}}. \quad (8)\end{aligned}$$

By solving Eqs. (1)–(5) and (8), we can get the Fermi energy of $Al_{0.25}Ga_{0.75}N$ as a function of the O concentration. As shown in Fig. 2, the Fermi energy of $Al_{0.25}Ga_{0.75}N$ distinctly increases with the increase of the O concentration. When the O concentration increases from 10^{13} cm^{-3} to 10^{20} cm^{-3}, the Fermi energy raises from 2.25 to 3.88 eV accordingly. Our result confirms that O_N causes auto *n*-type doping in $Al_xGa_{1-x}N$ alloys.

C. Effect of F doping on the Fermi level of $Al_{0.25}Ga_{0.75}N$

In this section, we take O concentrations of 10^{13} cm^{-3} and 10^{19} cm^{-3} as examples to investigate the effect of further F incorporation on the Fermi energy of $Al_{0.25}Ga_{0.75}N$.

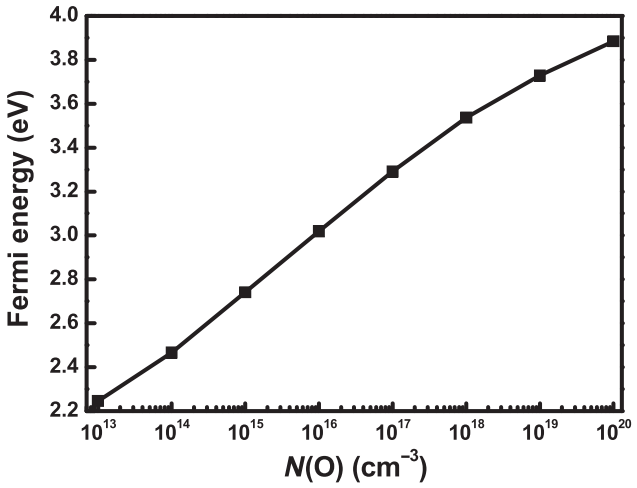

FIG. 2. The Fermi energy of $Al_{0.25}Ga_{0.75}N$ as a function of the O concentration at 1400 K.

When the concentration of O is 10^{13} cm^{-3}, we can see from Fig. 1 that the dominant defect configuration of F is F_N^{2+}. Therefore, we concentrate on the contributions of F_N, O_N, V_N, V_{Al}, and V_{Ga} to the Fermi energy of $Al_{0.25}Ga_{0.75}N$. Due to the existence of O_N, there are $N_N - N_{site-O_N} \approx N_N$ possible sites left, where N_N and N_{site-O_N} are the number of total N sites and O_N sites per volume, respectively. By solving Eqs. (1)–(5), we get the maximum F concentration is as low as 4.40×10^{11} cm^{-3} and the resulting Fermi energy is 2.33 eV. The low concentration of F_N^{2+} is caused by its high formation energy. Therefore, for $Al_xGa_{1-x}N$ with low concentration of O, it is difficult to dope F effectively. The low concentration of F exerts negligible effect on the host's Fermi energy.

When the concentration of O is 10^{19} cm^{-3}, we can see from Fig. 1 that the dominant defect configuration of F is F_i^-. Therefore, we focus on the contributions of F_i, O_N, V_N, V_{Al}, and V_{Ga} to the Fermi energy of $Al_{0.25}Ga_{0.75}N$. The formation energy of F_i in various charge states are given by

$$\begin{aligned}\Delta H_f(\mathrm{F}_i,0) &= E(\mathrm{F}_i,0) - E(\mathrm{host}) - [\mu_F + E(F)], \\ \Delta H_f(\mathrm{F}_i,+) &= \Delta H_f(\mathrm{F}_i,0) + \epsilon(0/+) - E_g + E_F, \\ \Delta H_f(\mathrm{F}_i,-) &= \Delta H_f(F_i,0) + \epsilon(0/-) - E_F. \quad (9)\end{aligned}$$

The concentrations of F_i in various charge states [$N(F_i,0)$, $N(F_i,+)$, and $N(F_i,-)$] are calculated by Eq. (5). The total concentrations of F_i is given by

$$\mathrm{N(F}_i) = \mathrm{N(F}_i,0) + \mathrm{N(F}_i,+) + \mathrm{N(F}_i,-). \quad (10)$$

With Eqs. (5), (9), and (10), we have

$$N(F_i,0) = \frac{16N(F_i)}{16 + 4e^{-[\varepsilon(0/+)-E_g+E_F]/k_BT} + 4e^{-[\varepsilon(0/-)-E_F]/k_BT}},$$
$$N(F_i,+) = \frac{4N(F_i)e^{-[\varepsilon(0/+)-E_g+E_F]/k_BT}}{16 + 4e^{-[\varepsilon(0/+)-E_g+E_F]/k_BT} + 4e^{-[\varepsilon(0/-)-E_F]/k_BT}},$$
$$N(F_i,-) = \frac{4N(F_i)e^{-[\varepsilon(0/-)-E_F]/k_BT}}{16 + 4e^{-[\varepsilon(0/+)-E_g+E_F]/k_BT} + 4e^{-[\varepsilon(0/-)-E_F]/k_BT}}. \quad (11)$$

By solving Eqs. (1)–(5) and (11), we can get the Fermi energy of $Al_{0.25}Ga_{0.75}N$ as a function of the F concentration. As shown in Fig. 3(a), when the concentration of F increases from $10^9 \sim 10^{18}$ cm^{-3}, the Fermi energy of the system slightly decreases from 3.73 to 3.71 eV. However, when the concentration of F increases from 10^{18} cm^{-3} to 10^{19} cm^{-3}, the Fermi energy decreases drastically from 3.71 to 2.22 eV. For $Al_{0.25}Ga_{0.75}N$ containing high concentration of O, positive charges mainly originate from ionized O_N^+ while negative charges mainly derive from thermally excited electrons (n_0) [Fig. 3(b)]. When the concentration of F increases to the value larger than 10^{18} cm^{-3}, the population of F_i^- becomes comparable or even larger than that of O_N^+ or n_0. The increase of the population for F_i^- gives rise to the decrease of the Fermi energy.

D. Effect of F on the performance of $Al_xGa_{1-x}N$/GaN HEMTs

In this section, we discuss the effect of F on the performance of $Al_xGa_{1-x}N$/GaN HEMTs, which depends on both the conductivity of the $Al_xGa_{1-x}N$ layer and the concentration of F. For $Al_xGa_{1-x}N$/GaN HEMTs with unintentionally doped $Al_xGa_{1-x}N$ layer with well-controlled low O concentration, F is incorporated as F_N^{2+}. The high formation energy of F_N^{2+} results in the low concentration of F_N^{2+} that changes neither the Fermi energy nor the shape for the CB of the $Al_xGa_{1-x}N$ layer. After F incorporation, the band diagram of the $Al_xGa_{1-x}N$/GaN heterostructure does not change, as shown in Fig. 4(a). Therefore, the low concentration of F_N^{2+} exerts negligible effect on the performance of $Al_xGa_{1-x}N$/GaN HEMTs.

For $Al_xGa_{1-x}N$/GaN HEMTs with unintentionally doped $Al_xGa_{1-x}N$ layer with high O concentration, the $Al_xGa_{1-x}N$ layer is *n*-type and F mainly presents as F_i^-. The concentration of F is the highest at the surface of the $Al_xGa_{1-x}N$ layer. With the increase of the distance from the surface, the depth profile distribution of F takes on a Gaussian distribution [8]. After incorporation of F with moderate concentration, the concentration of F is smaller than that of O_N^+ or n_0 in the $Al_xGa_{1-x}N$ layer. The Fermi energy of the $Al_xGa_{1-x}N$ layer basically keeps the same while the CB of the $Al_xGa_{1-x}N$ layer is raised because of F_i^-. The raise of the CB throughout the $Al_xGa_{1-x}N$ layer caused by F_i^- is denoted by R_F. For the CB near the surface

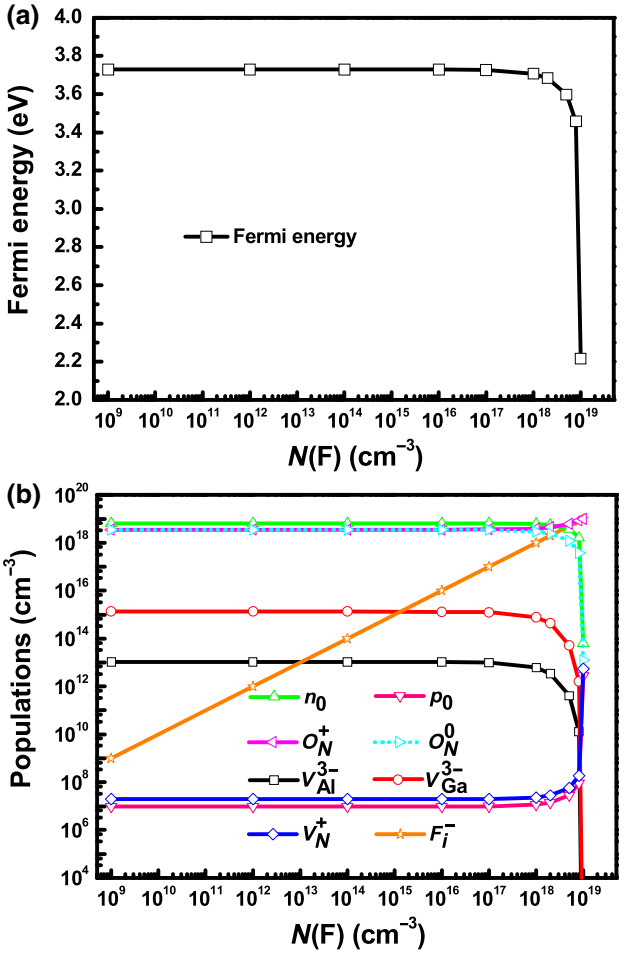

FIG. 3. (a) The Fermi energy of $Al_{0.25}Ga_{0.75}N$ with O concentration of 10^{19} cm^{-3} as a function of the F concentration at 1400 K. (b) In $Al_{0.25}Ga_{0.75}N$ with O concentration of 10^{19} cm^{-3}, the populations of n_0 (green), p_0 (pink), O_N^+ (magenta), O_N^0 (cyan), V_{Al}^{-3} (black), V_{Ga}^{-3} (red), V_N^+ (blue), and F_i^- (orange) as functions of the F concentration at 1400 K.

of the $Al_xGa_{1-x}N$ layer, the metal contact pins the CB. The resulting band diagram is shown in Fig. 4(b). In this case, the CBM of the $Al_xGa_{1-x}N$ layer is raised above the Fermi level. Therefore, the V_{th} is positively shifted while the surface potential and the Schottky barrier height essentially keeps the same after F incorporation.

For $Al_xGa_{1-x}N$/GaN HEMTs with the unintentionally doped $Al_xGa_{1-x}N$ layer with high O concentration, when the concentration of incorporated F_i^- becomes higher, we divide the $Al_xGa_{1-x}N$ layer into two regions to discuss the effect of F on the performance of $Al_xGa_{1-x}N$/GaN HEMTs: one with high F concentration near the surface (H) and the other with moderate F concentration away from the surface (M) [Fig. 4(c)]. The F_i^- throughout the $Al_xGa_{1-x}N$ layer raises the CB by R_{F_H}. In the M region, the moderate F concentration exerts negligible effect on the Fermi energy. However, the high F concentration in the H region

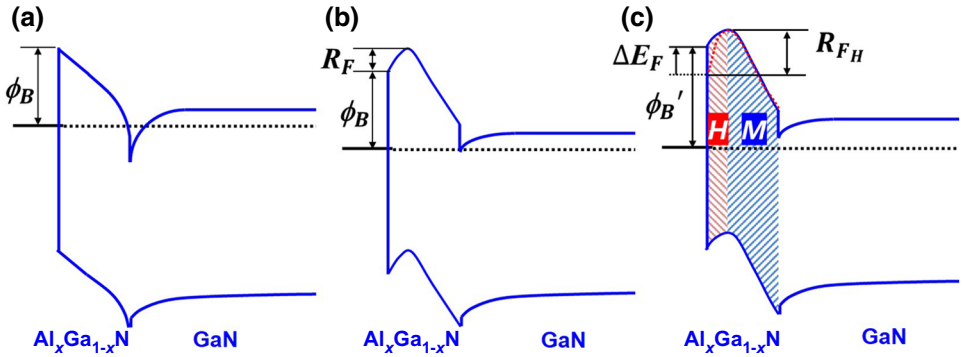

FIG. 4. Schematic band diagram of the $Al_xGa_{1-x}N/GaN$ heterostructure with F doping where the $Al_xGa_{1-x}N$ layer is (a) unintentionally doped with well-controlled low O concentration, (b) unintentionally doped with high O concentration and the concentration of F is moderate, (c) unintentionally doped with high O concentration and the concentration of F is high. The characters "H" and "M" indicate the high F-concentration region and the moderate F-concentration region, respectively.

decreases the Fermi energy of $Al_xGa_{1-x}N$ by ΔE_F, which raises the CB of H region by ΔE_F. Therefore, we can conclude that the shift of V_{th} results from R_{F_H}. The decrease of the Fermi energy of the H region $(-\Delta E_F)$ explains the slight increase of the surface potential and Schottky barrier height observed in the experimental research [18].

IV. CONCLUSION

In conclusion, we systematically study the defect physics of F in $Al_{0.25}Ga_{0.75}N$, and reveal the mechanism for the change of the electronical performance of $Al_xGa_{1-x}N/GaN$ HEMTs after F doping. We confirm that O will dope GaN and $Al_xGa_{1-x}N$ alloys to be *n*-type. If O is present in significant quantities in GaN and $Al_xGa_{1-x}N$ alloys, it results in unintentional *n*-type conductivity. For $Al_{0.25}Ga_{0.75}N$ with low O concentration, whose Fermi level lies in the midgap, the dominant defect configuration is F_N^{2+}. The effect of low concentration of F_N^{2+} exerts negligible effect on the Fermi energy of $Al_xGa_{1-x}N$ and the performance of the $Al_xGa_{1-x}N/GaN$ HEMT. For *n*-type $Al_{0.25}Ga_{0.75}N$ with unintentionally induced O, when the concentration of F is lower than that of O_N, the effect of F_i^- on the Fermi energy is negligible. Once the concentration of F becomes comparable or even larger than that of ionized O, the Fermi energy of $Al_xGa_{1-x}N$ decreases rapidly with the increase of the F concentration. As to the mechanism for the change of the electrical performance of $Al_xGa_{1-x}N/GaN$ HEMTs after F doping, we find that the positive shift of V_{th} after F doping is only achievable for $Al_xGa_{1-x}N/GaN$ HEMTs with the *n*-type $Al_xGa_{1-x}N$ layer. The changes of the surface potential and Schottky barrier height depend on the concentration of incorporated F. Only when the concentration of F is higher than that of *n*-type dopants, F begins to increase the surface potential and the Schottky barrier height.

ACKNOWLEDGMENTS

We are grateful to Professor Su-Huai Wei at Beijing Computational Science Research Center for insightful discussion. This work was supported by National Natural Science Foundation of China (Grant No. 61604141), Science Challenge Project (Grants No. TZ2016003, No. TZ2018003) and China Postdoctoral Science Foundation (Grant No. 2016M592700). National Supercomputer Center in Tianjin is acknowledged for computational support.

[1] P. P. Umesh, K. Mishra, and Y. F. Wu, AlGaN GaN HEMTs—An overview of device operation and applications, Proc. IEEE **90**, 1022 (2002).
[2] J. Zúñiga-Pérez, V. Consonni, L. Lymperakis, X. Kong, A. Trampert, S. Fernández-Garrido, O. Brandt, H. Renevier, S. Keller, K. Hestroffer, M. R. Wagner, J. S. Reparaz, F. Akyol, S. Rajan, S. Rennesson, T. Palacios, and G. Feuillet, Polarity in GaN and ZnO: Theory, measurement, growth, and devices, Appl. Phys. Rev. **3**, 041303 (2016).
[3] S. Dimitrijev, J. Han, H. A. Moghadam, and A. Aminbeidokhti, Power-switching applications beyond silicon: status and future prospects of SiC and GaN devices, MRS Bull. **40**, 399 (2015).
[4] K. J. Chen and C. Zhou, Enhancement-mode AlGaN/GaN HEMT and MIS-HEMT technology, Phys. Status Solidi A **208**, 434 (2011).
[5] K. J. Chen, in *Power* GaN *Devices* (Springer, 2017), p. 273.
[6] Y. Cai, Y. Zhou, K. M. Lau, and K. J. Chen, Control of threshold voltage of AlGaN/GaN HEMTs by fluoride-based plasma treatment: from depletion mode to enhancement mode, IEEE Trans. Electron Devices **53**, 2207 (2006).
[7] K. J. Chen and M. Wang, Improvement of the off-state breakdown voltage with fluorine ion implantation in AlGaN/GaN HEMTs, IEEE Trans. Electron Devices **58**, 460 (2011).
[8] A. Basu and I. Adesida, Accumulation of fluorine in CF_4 plasma-treated AlGaN/GaN heterostructure interface: An

experimental investigation, J. Appl. Phys. **105**, 033705 (2009).

[9] X. Sun, Y. Zhang, K. S. Chang-Liao, T. Palacios, and T. P. Ma, *Impacts of Fluorine-Treatment on E-Mode* AlGaN-GaN *MOS-HEMTs* (IEEE IEDM, San Francisco, 2014), 438.

[10] A. Basu, V. Kumar, and I. Adesida, Study of fluorine bombardment on the electrical properties of AlGaN/GaN heterostructures, J. Vac. Sci. Technol. B **25**, 2607 (2007).

[11] G. Dagher, T. D. H. Nguyen, N. Péré-Laperne, J. Mimila-Arroyo, M. Lijadi, F. Jomard, C. Dupuis, N. Bardou, and J.-L. Pelouard, Electrical behavior of GaN-HEMT after fluoride plasma treatment, Phys. Status Solidi C **8**, 2416 (2011).

[12] J. Osvald, T. Lalinský, G. Vanko, Š Haščík, and A. Vincze, C–V characterization of SF_6 plasma treated AlGaN GaN heterostructures, Microelectron. Eng. **87**, 2208 (2010).

[13] C. Ma, H. Chen, C. Zhou, S. Huang, and L. Yuan, On-state critical gate overdrive voltage for fluorine-implanted enhancement-mode AlGaN/GaN high electron mobility transistors, J. Appl. Phys. **110**, 114514 (2011).

[14] K. J. Chen, *The Role of Fluorine Ions in* GaN *Heterojunction Transistors: Applications and Stability* (SPIE OPTO, San Francisco, 2011), 3.

[15] R. Kawakami, M. Niibe, Y. Nakano, T. Shirahama, S. Hirai, and T. Mukai, Comparison between AlGaN surfaces etched by carbon tetrafluoride and argon plasmas: Effect of the fluorine impurities incorporated in the surface, Vacuum **119**, 264 (2015).

[16] M. J. Wang, L. Yuan, C. C. Cheng, C. D. Beling, and K. J. Chen, Defect formation and annealing behaviors of fluorine-implanted GaN layers revealed by positron annihilation spectroscopy, Appl. Phys. Lett. **94**, 061910 (2009).

[17] A. Uedono, N. Yoshihara, Y. Zhang, M. Sun, D. Piedra, T. Fujishima, S. Ishibashi, M. Sumiya, O. Laboutin, W. Johnson, and T. Palacios, Vacancy clusters introduced by CF4-based plasma treatment in GaN probed with a monoenergetic positron beam, Appl. Phys. Exp. **7**, 121001 (2014).

[18] S. Huang, H. Chen, and K. J. Chen, Effects of the fluorine plasma treatment on the surface potential and Schottky barrier height of $Al_xGa_{1-x}N$/GaN heterostructures, Appl. Phys. Lett. **96**, 233510 (2010).

[19] J. H. Yang, W. J. Yin, J. S. Park, W. Metzger, and S.-H. Wei, First-principles study of roles of Cu and Cl in polycrystalline CdTe, J. Appl. Phys. **119**, 045104 (2016).

[20] J. Ma, J. Yang, and S.-H. Wei, Correlation between the electronic structures and diffusion paths of interstitial defects in semiconductors: The case of CdTe, Phys. Rev. B **90**, 155208 (2014).

[21] S.-H. Wei, Overcoming the doping bottleneck in semiconductors, Comp. Mater. Sci. **30**, 337 (2004).

[22] C. G. Van de Walle, First-principles calculations for defects and impurities: Applications to III-nitrides, J. Appl. Phys. **95**, 3851 (2004).

[23] C. Freysoldt, B. Grabowski, T. Hickel, J. Neugebauer, G. Kresse, A. Janotti, and C. G. Van de Walle, First-principles calculations for point defects in solids, Rev. Mod. Phys. **86**, 253 (2014).

[24] A. Janotti, E. Snow, and C. G. Van de Walle, A pathway to p-type wide-band-gap semiconductors, Appl. Phys. Lett. **95**, 172109 (2009).

[25] K. H. Hong, I. Hwang, H. S. Choi, J. Oh, J. Shin, U. I. Chung, and J. Kim, Impacts of fluorine on GaN high electron mobility transistors: Theoretical study, Phys. Status Solidi R **4**, 332 (2010).

[26] B. C. Chung and M. Gershenzon, The influence of oxygen on the electrical and optical properties of GaN crystals grown by metalorganic vapor phase epitaxy, J. Appl. Phys. **72**, 651 (1992).

[27] W. Seifert, R. Franzheld, E. Butter, H. Sobotta, and V. Riede, On the origin of free carriers in high-conducting n-GaN, Cryst. Res. Technol. **18**, 383 (1983).

[28] R. Wang, W. Tan, J. Zhang, F.-X. Chen, and S.-H. Wei, First-principles study of alloying effects on fluorine incorporation in $Al_xGa_{1-x}N$ alloys, J. Phys. D: Appl. Phys. **51**, 065108 (2018).

[29] C. G. Van de Walle, S. Limpijumnong, and J. Neugebauer, First-principles studies of beryllium doping of GaN, Phys. Rev. B **63**, 245205 (2001).

[30] A. Zunger, S.-H. Wei, L. G. Ferreira, and J. E. Bernard, Special Quasirandom Structures, Phys. Rev. Lett. **65**, 353 (1990).

[31] S.-H. Wei, L. G. Ferreira, J. E. Bernard, and A. Zunger, Electronic properties of random alloys: Special quasirandom structures, Phys. Rev. B **42**, 9622 (1990).

[32] J. Ma and S.-H. Wei, Bowing of the defect formation energy in semiconductor alloys, Phys. Rev. B **87**, 241201(R) (2013).

[33] G. Kresse and D. Joubert, From ultrasoft pseudopotentials to the projector augmented-wave method, Phys. Rev. B **59**, 1758 (1999).

[34] G. Kresse and J. Furthmüller, Efficient iterative schemes for ab initio total-energy calculations using a plane-wave basis set, Phys. Rev. B **54**, 11169 (1996).

[35] J. Heyd, G. E. Scuseria, and M. Ernzerhof, Hybrid functionals based on a screened Coulomb potential, J. Chem. Phys. **118**, 8207 (2003).

[36] H. J. Monkhorst and J. D. Pack, Special points for Brillouin-zone integrations, Phys. Rev. B **13**, 5188 (1976).

[37] S.-H. Wei and S. B. Zhang, Chemical trends of defect formation and doping limit in II-VI semiconductors: The case of CdTe, Phys. Rev. B **66**, 155211 (2002).

[38] J. H. Yang, S. Chen, H. Xiang, X. G. Gong, and S.-H. Wei, First-principles study of defect properties of zinc blende MgTe, Phys. Rev. B **83**, 235208 (2011).

[39] A. M. Kurakin, S. A. Vitusevich, S. V. Danylyuk, H. Hardtdegen, N. Klein, Z. Bougrioua, A. V. Naumov, and A. E. Belyaev, Quantum confinement effect on the effective mass in two-dimensional electron gas of AlGaN/GaN heterostructures, J. Appl. Phys. **105**, 073703 (2009).